Very long-term incision dynamics of big rivers

Jean-Louis Grimaud, Dominique Chardon, Anicet Beauvais

Very long-term incision dynamics of big rivers

Jean-Louis Grimaud[1, 2, 3, 4 *], Dominique Chardon[1, 2, 3], Anicet Beauvais[5]

[1] Université de Toulouse, UPS (OMP), GET,
14 avenue Edouard Belin, 31400 Toulouse, France

[2] CNRS, GET, 31400 Toulouse, France

[3] IRD, UR 234, GET, 31400 Toulouse, France

[4] now at St. Anthony Falls Laboratory,
University of Minnesota, Minneapolis, Minnesota, USA

[5] Aix Marseille Université, IRD, CNRS, CEREGE UM 34
BP 80 - 13545 Aix-en-Provence Cedex 4, France

Manuscript EPSL-D-14-00446

Submitted 24 April 2014

Revised 24 July 2014

*Corresponding author:

E-mail address: jgrimaud@umn.edu

Abstract

Constraining large-scale incision dynamics of shield and post-rift margin domains is key to understanding the sediment routing system over the overwhelming part of the continental surface. Based on dated and regionally correlated incision markers from West Africa, we reconstruct for the first time the entire paleo-long profiles of big rivers such as the Niger at ca. 24, 11 and 6 Ma, as well as the Eocene topography those rivers have dissected. The results provide boundary conditions and calibration for surface process models and paleodrainage dynamics. Though spatially and temporally variable, incision remained mostly below 10 m/my with a mean around 5 m/my. The spatial stability of both the river outlets and divides imposed maintenance or increasing concavity of the river long profiles through time, resulting from spatially contrasted adjustment of river segments bounded by recurrent lithogenic knickzones that persisted since 24 Ma. Drainages evolved preferentially by very slow slope decrease or uniform incision in between the stationary knickzones of evolving amplitude, with apparently no relation to base level change. Therefore, knickzone height or position may not simply reflect the transient response of big rivers to base level fall as predicted by stream-power incision river models. This may also challenge uplift histories of deep continental interiors retrieved from river long profiles inversion relying on such models. Very slow incision allowed amplification of the Hoggar hot spot swell and flexural uplift of the continental margin to be recorded by river long profiles, emphasizing the potential of big non-orogenic rivers as gauges of dynamic topography.

1. Introduction

Quantifying incision dynamics of large drainage basins over geological time scales is relevant to constraining long-term landform evolution processes and the responses of the sediment routing system to lithospheric deformation and climate change. Spatial and temporal variations in incision rates are mostly investigated through the study of longitudinal profiles of rivers as gauges of transient responses of landscapes to perturbations such as base level fall due to uplift. Such responses are modeled using stream-power equations and commonly integrate the formation and headward propagation of knickpoints as a mechanism of river long profile evolution (e.g., Whipple and Tucker, 1999; Crosby and Whipple, 2006; Jeffery et al., 2013). Based on such models, an inversion procedure of river long profiles has been implemented to estimate surface uplift magnitudes (Roberts and White, 2010; Paul et al., 2014). But studies of incision processes are mostly based on modeling and/or focus on active tectonic settings over short time scales (10^3-10^6 yr) and face a crucial lack of regional markers of past base levels that would allow calibrating or testing incision models on Pre-Quaternary geological time scales (10^6-10^8 yr). This is particularly exemplified in non-orogenic settings where erosion is so slow that it may rarely be detectable by low-temperature thermochronology methods over the Cenozoic (e.g., Beauvais and Chardon, 2013). Constraining large-scale incision dynamics in such settings is however key to understanding the long-term reactivity of the overwhelming part of the continental surface that supplied most of the world's passive margins and intracratonic sedimentary basins. In these tectonically "stable" contexts, river long profiles display series of major knickzones and are commonly convex downstream (Summerfield, 1991, 1996; Pazzaglia et al., 1998). These profiles pose the sizable challenge of knowing how and how fast their geometry has been acquired, how knickzones formed and evolved and what caused their convexities. If post-rift flexure of passive margins has been suggested as a cause of warping of downstream river segments (Gilchrist and Summerfield, 1990), the contributions of climatically induced sea level or erosion process changes and lithospheric deformation to the acquisition of non-orogenic river long profiles are still unclear (Summerfield, 1991; Schumm, 1993; Beauvais and Chardon, 2013).

For the first time, we reconstruct consecutive long profiles of big rivers over their entire length since the Eocene by using the exceptional geomorphic record of successive incision stages of the West African subregion. Successive paleoprofiles allow constraining evolving rivers shapes with an emphasis on the dynamics of knickzones and are used to calibrate large-scale patterns of incision rates for three time slices over the last 24 Ma. Anomalies in river profiles are also analyzed as proxies of long wavelength lithospheric deformation.

2. Geomorphic setting and incision chronology

West African drainage is organized mostly around the Guinean rise and the Hoggar and Jos topographic massifs (Figure 1a). The drainage of West Africa is governed by three major river systems: the Senegal, Volta and Niger and includes shorter rivers draining the seaward slope of the Guinean rise (Figure 1a). The river long profiles are characterized by long (> 50 km), low gradient sections (i.e., 0.1 to 2 ‰) separated by knickpoints, identified as short (< 30 km) reaches of steep gradient (> 1%; Figure 1b). Two major regional knickzones made of a series of knickpoints over > 50 km long river segments are recognized on most river profiles at ca. 50-100 m and 200-250 m elevation (Figures 1a and 1b).

West Africa is characterized by an exceptional sequence of stepped lateritic paleolandsurfaces (Figure 2), whose remnants are preserved throughout the subregion. Paleo-river long profiles were constructed by using the remnants of these paleolandsurfaces along the studied rivers (see below). In the following, the characteristics of the paleolandsurfaces are summarized after the works, among others, of Vogt (1959), Eschenbrenner and Grandin (1970), Burke and Durotoye (1971), Michel (1973), Grandin (1976), Boulangé et al. (1973), Boulangé and Millot (1988) and the syntheses of Beauvais et al. (2008), Burke and Gunnell (2008) and Beauvais and Chardon (2013).

Relicts of surface 1 are preserved on West African summits and numerous mesas. It is a low-relief surface, which is the end product of enhanced chemical weathering that started in the Late Cretaceous and culminated in the Early Eocene to form bauxites (Figure 2). This bauxite-capped Eocene landscape, also called hereafter the bauxitic surface, represents today's envelope of the West African topography. The following paleolandsurfaces are stepped below the bauxite remnants and mark successive incision stages of the bauxitic surface (Figure 2). Surface 2, the so-called Intermediate surface, characterizes a differentiated remnant landscape coated by a thick ferricrete sealing an in-situ formed weathering mantle (Figure 2). As opposed to surfaces 1 and 2, the following three paleolandsurfaces in the sequence are pediments (glacis in the French literature): the so-called high (surface 3), middle (surface 4) and low glacis (Figure 2). The glacis surfaces commonly carry reworked bedrock and lateritic fragments derived from surfaces 1 and 2 and were, together with their cover, weathered to various degrees. Because the low glacis did not develop uniformly throughout West Africa or is commonly connected to local base levels, it was not used for paleo-long profiles reconstructions. Consequently, "surface 5" was considered as the current river levels (Figure 2). Each paleolandsurface (1 to 5) is taken as the end product of an incision period (I to V, respectively; Figure 2). Our study focuses on incision periods III to V and allows visualizing the amount of dissection of the Eocene topography during erosion period II.

Age constraints on the shaping, weathering and abandonment of the successive paleosurfaces in the West African sequence were obtained from radiometric ^{39}Ar-^{40}Ar dating of supergene K-Mn oxides (i.e., cryptomelane) in the weathering profiles of each paleosurface from the Tambao type locality (Figure 1a) in Burkina Faso (synthesis in Beauvais and Chardon, 2013). Surface and core samples were taken at various elevations and depths spanning the altitudinal range of the paleolandsurfaces (Hénocque et al., 1998; Colin et al., 2005; Beauvais et al., 2008). Paleosurfaces 1 to 4 yielded ^{39}Ar-^{40}Ar age groups of 59 - 45, 29 - 24, 18 -11 and 7-6 Ma, respectively, the Oligocene and Mid-Miocene weathering periods being also recorded by Ar-Ar dates of supergene jarosite and alunite in Southern Mali weathering profiles (Vasconcelos et al., 1994). The lower limits of the radiometric age groups date the stabilization of the weathering front established by the end of chemical weathering periods that ultimately led to duricrusting of each paleosurface in connection with their local base level (Beauvais and Chardon, 2013). Therefore, ca. 45, 24, 11 and 6 Ma are interpreted as the maximum age of abandonment of each paleosurface by river incision due to climate switches from humid to seasonally dry (Beauvais and Chardon, 2013; Figure 2a). In other words, the ages of ca. 45, 24, 11 and 6 Ma are the terminal ages of paleosurfaces 1, 2, 3 and 4 respectively (Figure 2a) bracketing the incision periods separating those paleosurfaces.

3. Method

We construct rivers paleo-long profiles based on the identification and mapping of remnant of paleolandsurfaces S1 to S4 along the rivers courses over approximately 20 km-wide corridors. This protocol is motivated by the fact that surfaces 2 and younger systematically dip towards those rivers (e.g., Figure 3). Our database of remnant lateritic paleosurfaces is that of Beauvais and Chardon (2013), which was extended to encompass the selected river corridors at about 400 stations. At each station, base level elevations corresponding to each paleolandsurface were obtained by projecting or extrapolating paleosurface remnant elevation(s) onto a vertical straight line above the current river trace (Figure 3b). Surface 1-bauxitic remnants were horizontally projected (Figure 3), sometime up to 50 km from the river. Inselberg tops with higher elevation than that of surface 2 relicts provide a minimum elevation for the bauxitic surface and were also projected horizontally. Surface 2 relicts commonly encompass altitudinal ranges on the slopes of bauxitic mesas (e.g., Figure 3b). The maximal and minimal elevations of surface 2 relict(s) were horizontally projected to reflect the amplitude of its local relief at each station (Figure 3b). Glacis form as concave upstream valley sides of 0.2 to 10° in slope connected to the local base level (Grandin, 1976; Strudley et al., 2006; Strudley and Murray, 2007). Thanks to their duricrusted cover, remnants of glacis surfaces 3 and 4 have their original shape well preserved (e.g., Figure 3b). We therefore extrapolated the downslope shape of the glacis by picking points from their surface along a down-dip section towards the river (Figure 3b) and exponentially fitting those points using formula:

$$z = z_0 + H \exp^{-(x/\sigma)} \quad (1)$$

where x is the horizontal distance to the river, z is the elevation. z_0 is the minimum elevation of the considered geomorphic surface. σ is a measure of the exponential reduction of elevation, i.e. a measure of inverse concavity, and H is a constant set by the elevation amplitude of pediments surface. Base levels 3 and 4 elevation is calculated at the river. Elevation error is estimated using the derivative:

$$\mathrm{d}z = \mathrm{d}z_{srtm} + \mathrm{d}z_0 + \exp^{-(x/\sigma_{op})}\, \mathrm{d}A + H_{op}\left(\frac{x}{\sigma_{op}^2}\right)\exp^{-(x/\sigma_{op})}\, \mathrm{d}\sigma \quad (2)$$

where $\mathrm{d}z_{srtm}$ is the absolute error of SRTM DEM (5.6 m in Africa ; Farr et al., 2007). σ index represents the inverse of concavity of the exponential fit and H_{op} and σ_{op} are the optimum values given by the interpolation. Distribution of σ_{op} is quasi-normal and centered on 300 (Figure 4), attesting to the repeatability of the glacis shape over the study area and justifying the use of the fit formula (equation 1). At most stations, the error induced by the extrapolation of glacis base levels is smaller than the data point size (Figure 3b and 5). This, together with the little skewed distribution of σ_{op} (Figure 4) shows that the extrapolated paleobase levels are robust. At stations where glacis remnants are not large enough to be confidently extrapolated, the lowest elevation of the remnant the closest to the river is horizontally projected.

Given the long projection distance of some bauxite relicts and the fact that the bauxitic surface has a regional relief (Chardon et al., 2006), the envelope topography of the Eocene landscape was drawn passing through surface 1 elevation data points (Figure 5). The curve joining the elevation of the lowest remnants of surface 2 has been drawn to represent the maximal elevation of rivers paleo-long profile 2 (Figure 5). Long profiles 3 and 4 were drawn from extrapolated surfaces 3 and 4 remnants or their projected lowest remnants. Modern profiles 5 were automatically extracted from the SRTM digital elevation model (Figure 5). Incision rates III, IV and V (representing time intervals 24-11, 11-6 and 6-0 Ma, respectively) were plotted along river profiles (Figure 5). Incision rates IV and V were obtained using base levels 3, 4 and 5 at each station by integrating the elevation error resulting from the extrapolation (Figure 5). Maximum values of incision rate III are derived from the difference between paleoprofiles 2 and 3.

Detection and qualification of steps on paleoprofiles depend on data resolution. Analysis of the current and past long profiles allows defining knickzones as < 90 km-long river segments of more than 1% slope between two longer adjoining linear segments of 0.1 to 2‰ slopes. Knickpoints, which are sharper by definition, are only rarely detectable on the reconstructed profiles. Although the river profiles have undergone long-wavelength distortion (section 5.2), their differential elevations constitute a meaningful estimate of incision. Likewise, comparing the relative geometry of short (<100 km) successive paleo-river segments is appropriate and relevant.

4. Results

We separate the studied river systems into four groups according to their location in the West African drainage (Figure 1). Group A includes the rivers draining the northwestern slope of the Guinean rise (Senegal and Gambia). Group B includes the short rivers draining the southern slope of the Guinean rise (Kakrima and Mano). Group C comprises the long southern rivers (Bandama, Comoé and Volta) and group D corresponds to the Niger drainage. The Niger River is divided in two segments (High and Low Niger) on both sides of the Niger inland delta (Figure 1). To facilitate the description of results, we show one representative example for each group (i.e. the Senegal, Kakrima, Volta and Niger main stream channels for groups A, B, C and D respectively) on Figure 5. The entire set of reconstructed profiles can be found in the data repositories.

4. 1. Overall profiles shape and early drainage reorganization

Past and modern long profiles of group A have a nearly straight, very low gradient slope across the Senegalo-Mauritanian basin (Figure 5a). Upstream parts of the profiles are steeper, generally stepped, with an increased slope (up to 0.7 ‰) for rivers draining the Western Guinean rise. Group B comprises the shortest rivers with paleo- and modern long profiles that have the steepest mean slopes (> 2 ‰) and are the most stepped (Figure 5b). The paleo and modern profiles of the Volta (group C) and Low Niger (group D) reveal a two-stage evolution. Indeed, the envelope of surface 1 underlines a divide whose crest lies between 200 and 750 km inland (Figures 5c and 5d). Groups C and D rivers have incised this divide mostly during incision period II. This, together with the overall evolution of group A and B rivers indicates drainage reorganization during period II resulting from the dissection of an Eocene marginal upwarp that survived or was rejuvenated in the Guinean rise (Beauvais and Chardon, 2013). This rearrangement involved capture of pre-45 Ma internal drainages by at least the Volta and Low Niger. More generally, depressions in the envelope of surface 1 (e.g., Figure 5c) are indicative of transverse paleovalleys before drainage rearrangement and/or second-order captures during rearrangement (see also data repositories). The fact that the post-rearrangement, 24 Ma old surface 2 systematically dips towards the current main drains warrants calibration of post 24 Ma incision.

Group C profiles 2 to 5 show a nearly parallel evolution. They are made of straight, low slope (< 0.1 - 0.3 ‰) segments hundreds of kilometers long, which are separated by knickzones, notably those highlighted on Figure 1. Profiles 2 to 5 converge and merge towards the coast downstream of the lower regional knickzone (Figure 5b). The High Niger River shows strongly concave paleo and modern profiles (Figure 5e), whereas post-surface 1 Low Niger profiles have low and slightly convex slopes diverging downstream (Figure 5d). Paleo long profiles reveal that knickzones on modern profiles have persisted since at least profile 3 (Figure 5).

Analysis of geological maps shows that those recurrent knickzones coincide with lithological contrasts expressed in the topography (Figure 5). Two main contrasts are distinguished, those related to steep contacts between greenstone belts and their adjoining granite-gneiss terrains and those formed across tabular sandstones. In the first case, the knickzone horizontally encompasses the along-river width of a greenstone belt or the lower limit of the knickzone coincides with the contact between a wide greenstone belt and granitogneisses. In the second case, the most common configuration is the lower limit of the knickzone coinciding with the basal unconformity of the sandstones.

4. 2. Northwestern rivers (group A)

On group A rivers, post-surface 2 incision generally increases from the extremities towards the central part of the profiles resulting in an increasing concavity of the profiles through time. This is particularly the case for incision IV, and, to a lesser extent, incision III (Figure 5a). In the Guinean rise, profiles 3 and 4 show mainly convex segments, with local high incision rates (up to 20 m/my) for period IV (Figure 5a). Overall, incision is rather uniform during period III and becomes more localized afterwards though accompanied by a decrease of the incision rates. Incision V is locally enhanced (up to 10 m/my) by the formation of new knickzones on profile 5 (Figure 5a).

4. 3. Short southern rivers (group B)

Long (> 100 km) segments of paleoprofiles 2, 3 and 4 are convex (Figure 5b). The stepped character of the profiles is accentuated through time by the apparition of shorter convex segments, particularly during incisions IV and V. Post surface 2 incisions tend to increase from the extremities towards the central part of the profiles, with locally enhanced incision during incisions IV and V that led to the formation of the modern knickzones (Figure 5b). This attests to a heterogeneous incision pattern during these periods (2 to 25 m/my), as opposed to rather distributed incision during period III (about 10 m/my in average). Incision gradients are located in between knickzones, the highest peaks being located mainly upstream. Elevation difference between surface 1 and the modern profiles implies a maximum incision of the slope of the Guinean rise of the order of 400 m (but equivalent to only 9 m/my over the last 45 Ma) (Figure 5b).

4. 4. Long southern rivers (group C)

The overall geometry of river long profiles has been acquired since the establishment of profiles 2. The two regional knickzones systematically coincide with lithological contrasts and occurred at least since profile 3 (Figure 5c). A mean cumulated incision of less than 50 m is derived from parallel and close profiles 3 to 5. Rivers show a rather parallel evolutionary pattern of profiles 2 and 3 along the central river segment comprised between the two regional knickzones (Figure 5c). This is indicative of a rather distributed incision III of ca. 7 m/my. By contrast, lower gradient of profile 2 diverges from profile 3 downstream of the upper regional knickzone and the two profiles tend to merge towards the coast (Figure 5c). Overall, eastern rivers of group C such as the Volta become increasingly stepped with time (Figure 5c).

4. 5. Niger River (group D)

Although the recurrence of the two regional knickzones is not readily documented along the Low Niger, the overall pattern of profiles 2 to 5 is roughly comparable to that of the Volta, with a diversion of the profiles downstream of the inland delta (e.g., comparison of Figures 5c and 5d). This attests to an increase in Neogene incision(s) downstream the inland delta. The overall long wavelength convexity of profiles 3 and 4 is documented between 200 and 1200 km (Figure 5d). Nearly parallel profiles 2 to 4 converge within the Iullemmeden basin. A single knickzone may be documented on profile 3 (ca. 450 km) and none may be detected on profile 4 (Figure 5d). But this may be due to the low resolution of our dataset downstream of the Iullemmeden basin. A two-step knickzone occurs on the modern profile between 800 and 1000 km (Figure 5d). Incision period V created high local relief compared to that of period IV, particularly downstream of the lower regional knickzone (e.g., Figure 5d). Incision V becomes limited approaching the inland delta and the coast (< 5 m/my) and increases towards the central part of the profiles, with the highest incision rates downstream of the two-step knickzone of profile 5 (ca. 10 m/my during periods II, IV and V; Figure 5d).

Paleo long river profiles of the High Niger (Figure 5e) are comparable to those of the Senegal (group A, e.g., Figure 5a). All the profiles converge downstream and merge entering the inland delta, which is preceded by a knickzone 400 km upstream (Figure 5e). Profiles 2 to 5 may be divided in two segments i.e., a lower, ca. 1000 km long and low gradient segment of parallel profiles and an upper, very steep and short segment within the Guinean rise (Figure 5e). Most of the incision along the High Niger took place during period II (locally more than 15 m/my). Incision rates III to V are remarkably low and uniform along the lower segment (< 6 m/my) and may locally attain 15 m/my in the Guinean rise (Figure 5e). The overall tendency of the upper Niger is an increase in the concavity of river profiles.

5. Interpretation and discussion

5.1. Incision dynamics and river profiles evolution

The present analysis shows that the overall shape of river profiles was acquired at least since ~11 Ma, and most probably ~24 Ma (Figure 6). The overall concavity of the successive river long profiles increased over the Neogene as a result of the pinning down of their two extremities (Figure 6). This attests to the horizontal stability of the divides and efficient adaptation to relative sea level change at the coast over the

Neogene. This very long-term divide stability, which has also been documented for the Southeastern margin of Australia (e.g., Young, 1989) contrasts with the view of drainage networks as “permanently” reorganizing in comparable passive margin contexts (Willett et al., 2014). We suggest that following drainage rearrangement (section 4.1), local relief and regional topography of West Africa acquired by the end of erosion period II had attained a threshold preventing divide migration after the Oligocene. Neogene divide stability over West Africa implies long-term stable geometry of drainage basins, which has major implications for understanding source-to-sink systems (Grimaud et al., 2014). This stability is reflected by low incision rates through space and time with more than 75 % of the data below 10 m/my and medians and means between 3 and 15 m/my (Figure 7). The last incision period would have recorded the smallest incision rates. Highest incision rates correspond to the steepest rivers draining the Guinean rise (groups A and B; Figure 7; upper Niger; Figure 5e), suggesting a control of potentially old, large-scale reliefs on incision heterogeneities (Beauvais and Chardon, 2013). To summarize, the present work provides constraints on boundary conditions and incision rates for large-scale surface process models in “stable” continental environments over geological time scales.

Our results reveal the long lasting maintenance of lithogenic knickzones along most rivers for at least ~11 my and most probably 24 my (Figure 6). Similar recurrent knickzones were documented in the comparable morphotectonic context of Eastern Australia (Bishop et al., 1985; van der Beek and Bishop, 2003). The concavity and stepped character of West African river long profiles have been amplified since the Early Neogene by very slow, non-uniform and unsteady incision in between stationary knickzones (Figures 5 and 6). Type-evolutionary patterns of rivers segments comprised between stationary knickzones are shown on Figure 8. Parallel evolution by strict uniform incision (Figure 8a) is characteristic of the High Niger River since 24 Ma (Figures 5e and 6d). Such an evolution is also locally observed on segments of the Low Senegal, Volta and Low Niger (Figure 5a, 5c and 5d). In all cases, strict uniform incision is systematically of very low rate (< 5 m/my). Strict downstream rejuvenation (Figure 8b) is not recorded by any of the studied rivers (Figure 5). Instead, knickzones may be created by differential incision (Figure 8c), as exemplified by the Senegal and Low Niger (at 1600-1800 km in Figure 5a and 400-500 km and 800-1000 km in Figure 5d). However, most knickzones in West Africa have been amplified or smoothed instead of having been created since 24 Ma (Figure 5). This resulted in slope lowering of most river segments, reflecting finite incision gradients along those segments (Figure 8d). This situation is best exemplified along the Senegal (at 1000-1200 km), Kakrima (at 100-300 km), Volta (600-800 km) and Low Niger (at 400-800 km and 1700-2000 km) (Figure 5).

The above analysis indicates that knickzones do not and did not separate downstream rejuvenated from upstream relict portions of the landscape, which is implicit in models of river long profile evolution by pure knickzone retreat, particularly that originally popularized by King (1948) in the African context. River segments bounded by recurrent lithogenic knickzones evolved apparently independently from each other by preferential slope decrease or uniform incision in between nodes made by pinned knickzones of evolving amplitude. This indicates that large non-orogenic drainage basins evolve through very slow (< 10 m/my) and non-uniform incision patterns that do not respond in a simple way to relative sea level change, to the exception of their lowermost reaches i.e., group C and D rivers during period IV (Figures 5 and 6, see below). In other words, repercussion of a major relative sea level drop is not likely to be recorded at a large distance from the coast in such drainages.

This warrants caution in using knickzones' height as a gauge of discrete uplift and figuring river profile response to uplift by headward propagation of such knickzones using stream-power river incision models. Accordingly, uplift histories retrieved from river profiles inversion procedures based on such models could be challenged, particularly those obtained for reliefs of the deep interior of the African continent (see Roberts and White, 2010 and Paul et al., 2014). As opposed to uplift, our results would argue for a dominant control of climate-driven erosion processes on incision dynamics of big non-orogenic drainages over geological time scales (Beauvais and Chardon, 2013).

5.2. Anomalies in river profiles and lithospheric deformation

Long wavelength (300 - 500 km long) upward convex segments of modern river profiles define a large domain comprising the Upper Volta and upper part of the Low Niger drainages (Figures 6c, 6d and 9). Our field observations and digital topographic data further indicate that this area coincides with portions of the Niger drainage that have incised their lowermost terrace. The convex river segments do not exceed 50 m in amplitude and are interpreted to reflect active transient adjustment by enhanced incision. The dynamics of two other major segments of the Niger and Volta drainage have been modified in the recent geological past. Indeed, the lower portion of the High Niger and the Gondo flew to NE before becoming alluvial plains (i.e., internal deltas) around the end of the Pliocene (Figure 9). These changes in river dynamics may result from slope decrease of those NE flowing drains. Both the upward convex river segments and internal deltas are interpreted to respond to southwestward growth of the Hoggar swell, which would be comparable to the lateral propagation of an active anticline (Keller et al., 1999), the direction and sense of propagation being determined by the northeastward displacement of the African plate with respect to the Hoggar plume and/or to asthenospheric flow under the plate (Figure 9). Swell growth would induce slope decrease on the drains flowing towards the propagating swell to create internal deltas, whereas drains flowing across the propagating swell undergo enhanced incision to keep pace with growing uplift. The area of active uplift (Figure 9) mimics the domain of positive dynamic topography expected from mantle circulation models of Forte et al. (2010), reinforcing the causal link suggested here between mantle dynamics and river profiles evolution.

Long wavelength (500 - 1000 km) convexities of the lower part of river profiles 2 to 4 are documented for drainages C and D (Figures 6c and 6d). For group C, convexity seems to increase with time (from profile 3 to profile 2) and has maximum amplitude of ca. 100 m and a wavelength of ca. 500 km. This convexity is replaced on the current profile by the lower regional knick zone and a concave lowermost portion of the rivers (Figure 6c). Warping is also documented on the lower Niger particularly on nearly parallel profiles 2 and 3, with a ca. 200 m amplitude and 1000 km wavelength convexity (Figure 6d). The convexity amplitude of profile 4 is much lower, indicating that profiles 2 and 3 underwent warping mainly before 6 Ma. The last erosion period (i.e., post 6 Ma) is also characterized by the creation of the major (double) regional knickzone and the acquisition of a concave lowermost profile (Figure 6d). Warping and post-6 Ma rejuvenation by knickzone creation of the lowermost portion of group C and D rivers are interpreted to result from flexural uplift of the continental margin (e.g., Gilchrist and Summerfield, 1990). Flexure was enhanced by (i) the narrowness of the two transform segments of the margin in this area (Figure 9), (ii) high and increasing Neogene clastic sedimentation rates at its foot (Séranne, 1999; Jermannaud et al., 2010) and (iii) onshore denudation (Beauvais and Chardon, 2013). The 500-1000 km wavelength of the flexure is too large to reflect only warping across a steep margin and is typical of asthenospheric-scale processes (e.g., McKenzie and Fairhead, 1997). We suggest that flexural uplift of the margin combined with the growth of the Hoggar swell (this work) and/or with the uplift of the continent (e.g., Burke, 1996) to produce such a wavelength.

5.3. Open questions

Creation or amplification of major knickzones achieves post 6 Ma rejuvenation of the warped lower portion of rivers flowing to the transform portions of the West African margin (Figure 6). The contribution, if any, of the Quaternary eustatic cycles to the creation of those knickzones may not be evaluated and whether these knickzones are actively migrating and/or evolve by knickpoint retreat should be the focus of future research. Knickpoint retreat is inferred to have been instrumental in the Plio-Pleistocene rejuvenation of the Appalachian landscape in a passive margin context comparable to that of West Africa (Gallen et al., 2013). Upstream West African drainage did not evolve by large wave(s) of headward migrating knickzones but our results are based on very long term measurements that may have averaged discrete periods of fast incision (Gardner et al., 1987). Hence, they do not allow testing whether knickpoint retreat process actually contributed to shaping individual river segments bounded by recurrent knickzones.

Likewise, documented distortion of portions of past river profiles poses the issue of whether rivers maintained their concavity against upwarping of abandoned base level markers or increased their overall concavity from more convex states. In the case of the lower reaches of group C and D rivers having undergone marginal flexural uplift, the first situation would clearly apply. The second situation could apply to the rest of the drainage with the noticeable exception of the northern slope of the Guinean rise (group A rivers; Figures 5a and 6a). But in absence of independent geological constraints on the potential relative uplift of the rise during the Cenozoic, it is not possible to evaluate its impact on the acquisition of long river profiles of West Africa.

6. Conclusions

The spatial analysis of dated and regionally correlated incision markers allows calibrating incision dynamics of big West African rivers over the last 45 my and quantifying the evolution of their long profiles since 24 Ma. Incision rates are distributed spatially and remained below 10 m/my and mostly below 5 m/my. Spatial stability of both the outlets and divides of the rivers since 24 Ma imposed increasing overall concavity of their long profiles, which was achieved by contrasted adjustment of river segments separated by persistent lithogenic knickzones. River segments evolve by preferential slope decrease or uniform incision in between nodes defined by the pinned knickzones of evolving amplitude. Therefore big non-orogenic rivers do not respond simply to relative sea level change, which is unlikely to be recorded far inland in the form of purely retreating knickzones. Accordingly, knickzone height or position on such rivers are not obvious gauges of base level fall and caution is required in retrieving regional uplift histories of deep continental interiors from river long profiles inversion procedures. Rather uniform and slow incision of large non-orogenic drainage basins allows distortion and anomalies in river profiles to record subtle long wavelength surface uplift due to hot spot swell growth and flexure of continental margins, emphasizing their potential as gauges of dynamic topography.

Acknowledgments

This work was funded by the ANR TopoAfrica (ANR-08-BLAN-572 0247-02), the CNRS and WAXI. We thank S. Carretier, S. Bonnet, P. van der Beek and G. Hérail for fruitful discussions and Ph. Dussouillez for support. We are indebted to F. Pazzaglia for very constructive reviews. The manuscript benefited from comments by K. Burke and anonymous reviewers. We acknowledge AMIRA International and the industry sponsors, including AusAid and the ARC Linkage Project LP110100667, for their support of the WAXI project (P934A) as well as the Geological Surveys/Departments of Mines in West Africa as sponsors in kind of WAXI.

References

Beauvais, A., Chardon, D., 2013. Modes, tempo and spatial variability of Cenozoic cratonic denudation: The West African example. Geochem. Geophys. Geosyst. 14, 1590–1608, doi:10.1002/ggge.20093.

Beauvais, A., Ruffet, G., Hénocque, O., Colin, F., 2008. Chemical and physical erosion rhythms of the West African Cenozoic morphogenesis: The ^{39}Ar-^{40}Ar dating of supergene K-Mn oxides. J. Geophys. Res. 113, F04007, doi:10.1029/2008JF000996.

Bishop, P., Young, R.W., McDougall, I., 1985. Stream profile change and longterm landscape evolution. Early Miocene and modern rivers of the East Australian highland crest, central New South Wales, Australia. J. Geol. 93, 455-474.

Bishop, P., 1985. Southeast Australian late Mesozoic and Cenozoic denudation rates: A test for late Tertiary increases in continental denudation. Geology 13(7), 479-482.

Boulangé, B., Delvigne, J., Eschenbrenner, V., 1973. Descriptions morphoscopiques, géochimiques et minéralogiques des faciès cuirassés des principaux niveaux géomorphologiques de Côte d’Ivoire. Cah. ORSTOM, sér. Géol. V(1), 59-81.

Boulangé, B., Millot, G., 1988. La distribution des bauxites sur le craton ouest-africain. Sci. Géol. Bull. 41(1), 113-123.

Burke, K., 1996. The African Plate. S. Afr. J. Geol. 99, 339-409.

Burke, K., Gunnell, Y., 2008. The African Erosion Surface: A Continental-Scale Synthesis of Geomorphology, Tectonics, and Environmental Change over the Past 180 Million Years. Geol. Soc. Am. Mem. 201, 1-66.

Burke, K., Durotoye, B., 1971. Geomorphology and superficial deposits related to large Quaternary climatic variations in South Western Nigeria. Z. Geomorph. 15, 430–444.

Chardon, D., Chevillotte, V., Beauvais, A., Grandin, G., Boulangé, B., 2006. Planation, bauxites and epeirogeny: One or two paleosurfaces on the West African margin? Geomorphology 82, 273-282.

Colin, F., Beauvais, A., Ruffet, G., Hénocque, O., 2005. First $^{40}Ar/^{39}Ar$ geochronology of lateritic manganiferous pisolites: Implications for the Palaeogene history of a West African landscape. Earth Planet. Sci. Lett. 238(1-2), 172-188. doi: 10.1016/j.epsl.2005.06.052.

Crosby, B.T., Whipple, K.X., 2006. Knickpoint initiation and distribution within fluvial networks: 236 waterfalls in the Waipaoa River, North Island, New Zealand. Geomorphology 82, 16-38.

Eschenbrenner, R., Grandin, G., 1970. La séquence de cuirasses et ses différenciations entre Agnibiléfrou et Diébougou (Haute-Volta). Cah. ORSTOM, Sér. Géol. 2(2), 205-246.

Farr, T.G., Rosen, P.A., Caro, E., Crippen, R., Duren, R., Hensley, S., Kobrick, M., Paller, M., Rodriguez, E., Roth, L., Seal, D., Shaffer, S., Shimada, J., Umland, J., Werner, M., Oskin, M., Burbank, D., Alsdorf, D., 2007. The Shuttle Radar Topography Mission. Rev. Geophys. 45, RG2004.

Forte, A.M., Quéré, S., Moucha, R., Simmons, N.A., Grand, S.P., Mitrovica, J.X., Rowley, D.B., 2010. Joint seismic–geodynamic-mineral physical modelling of African geodynamics: A reconciliation of deep-mantle convection with surface geophysical constraints. Earth Planet. Sci. Lett. 295, 329-341.

Gallen, S.F., Wegmann, K.W., Bohenstielhl, D.R., 2013. Miocene rejuvenation of topographic relief in the Southern Appalachians. GSA Today 23(2), 4-10, doi:10.1130/GSATG163A.1.

Gardner, T.W., Jorgensen, D.W., Shuman, C., and Lemieux, C.R., 1987. Geomorphic and tectonic process rates: Effects of measured time interval, Geology 15(3), 259-261, doi:10.1130/0091-7613(1987)15<259:GATPRE>2.0.CO;2.

Gilchrist, A.R., Summerfield, M.A., 1990. Differential denudation and flexural isostasy in formation of rifted-margin upwarps. Nature 346, 739-742.

Grandin, G., 1976. Aplanissements cuirassés et enrichissement des gisements de manganèse dans quelques régions d'Afrique de l'Ouest. Mém. ORSTOM 82, Paris, France.

Grimaud, J.-L., Chardon, D., Rouby, D., Beauvais, A., 2014. Quantifying denudation of the West African passive-transform margin: implications for Cenozoic erosion budget of cratons and source-to-sink systems. Geophys. Res. Abstr. 16, EGU2014-9913.

Hénocque, O., Ruffet, G., Colin, F., Féraud G., 1998. ^{40}Ar/^{39}Ar dating of West African lateritic cryptomelanes. Geochim. Cosmochim. Acta 62(16), 2739-2756.

Jeffery, M.L., Ehlers, T.A., Yanites, B.J., Poulsen, C.J., 2013. Quantifying the role of paleoclimate and Andean Plateau uplift on river incision. J. Geophys. Res. Earth Surf. 118, 852-871. doi: 10.1002/jgrf.20055.

Jermannaud P., Rouby, D., Robin, C. Nalpas, T., Guillocheau, 2010. Plio-Pleistocene Sequence Stratigraphic architecture of the eastern Niger delta: a record of eustasy and aridification of Africa. Mar. Pet. Geol. 27, 810-821

Keller, E.A., Gurrola, L., Tierney, T.E., 1999. Geomorphic criteria to determine the direction of lateral propagation of reverse faulting and folding. Geology 27, 515-518.

King, L.C., 1948. On the age of African land-surfaces. Q. J. Geol. Soc. London 104, 439-459.

McKenzie, D., Fairhead, D., 1997. Estimates of the effective elastic thickness of the continental lithosphere from Bouguer and free air gravity anomalies. J. Geophys. Res. 102, 27523-27552.

Michel, P., 1973. Les bassins des fleuves Sénégal et Gambie : étude géomorphologique. Mém. ORSTOM 63, Paris, France.

Paul, J.D., Roberts, G.G., White, N., 2014. The African landscape through space and time. Tectonics 33(6), 898-935, doi:10.1002/2013TC003479.

Pazzaglia, F.J., Gardner, T.W., Merritts, D.J., 1998. Bedrock fluvial incision and longitudinal profile development over geologic time scales determined by fluvial terraces, in: J. Tinkler, Wohl, E. (Eds.), Rivers Over Rock: Fluvial Processes in Bedrock Channels, Geophys. Monogr. Ser., vol. 107. AGU, Washington, DC, pp. 207-235.

Roberts, G.G., White, N., 2010. Estimating uplift rate histories from river profiles using African examples. J. Geophys. Res. Solid Earth 115, B02406.

Schumm, S.A., 1993. River response to baselevel change: Implications for sequence stratigraphy. J. Geol. 101, 279-294.

Séranne, M., 1999. Early Oligocene stratigraphic turnover on the West Africa continental margin: a signature of the Tertiary greenhouse-to-icehouse transition? Terra Nova 11(4), 135-140.

Strudley, M.W., Murray, A.B., 2007. Sensitivity analysis of pediment development through numerical simulation and selected geospatial query. Geomorphology 88, 329-351.

Strudley, M.W., Murray, A.B., Haff, P.K., 2006. Emergence of pediments, tors, and piedmont junctions from a bedrock weathering–regolith thickness feedback. Geology 34, 805-808.

Summerfield, M.A., 1991. Global geomorphology; an introduction to the study of landforms. Longman Scientific & Technical, Harlow, UK.

Summerfield, M.A., 1996. Tectonics, geology and long-term landscape development, in: W.M. Adams, A.S. Goudie, R. Orme, A. (Eds.), The Physical Geography of Africa. Oxford University Press, Oxford, UK, pp. 1-17.

van der Beek, P., Bishop, P., 2003. Cenozoic river profile development in the Upper Lachlan catchment (SE Australia) as a test of quantitative fluvial incision models. J. Geophys. Res. 108(B6), 2309.

Vasconcelos, P. M., Brimhall, G. H., Becker, T. A., Renne, P. R., 1994. ^{40}Ar/^{39}Ar analysis of supergene jarosite and alunite: Implications to the paleoweathering history of the western USA and West Africa. Geochim. Cosmochim. Acta 58(1), 401-420.

Vogt, J., 1959. Aspects de l'évolution morphologique récente de l'ouest africain. Ann. Géog. Fr. 68, 367, 193-206.

Whipple, K.X., Tucker, G.E., 1999. Dynamics of the stream-power river incision model; implications for height limits of mountain ranges, landscape response timescales, and research needs. J. Geophys. Res. 104 (B8), 17661–17674, doi: 10.1029/1999JB900120.

Willett, S.D., McCoy, S.W., Perron, T.J., Goren, L., Chen C-Y., 2014. Dynamic reorganization of river basins. Science 343, 1248765, doi:10.1126/science.1248765.

Young, R.W., 1989. Crustal constraints on the evolution of the continental divide of eastern Australia. Geology 17, 528-530.

Figure captions

Figure 1. (a) Topography, drainage and selected geologic and geomorphic features of West Africa. Topography is derived from smoothing of the Shuttle Radar Topography Mission DEM to 5 km resolution. Thick grey lines labeled 1 and 2 refer to the lower and upper regional knickzones, respectively. Capital letters refer to the studied groups of rivers. A – northwestern rivers (long profiles shown in Figure 5a); B – short southern rivers (Figure 5b); C – long southern rivers (Figure 5c); D – Niger River (Figure 5d). (b) Modern long profiles of selected rivers. The lower and upper regional knickzones' elevation ranges are indicated by dark and light grey bands numbered 1 and 2, respectively.

Figure 2. Lateritic paleolandsurface sequence and incision chronology of West Africa (synthesized after Michel, 1973; Beauvais et al., 2008; Beauvais and Chardon, 2013).

Figure 3. Example of a typical field station used to estimate local paleo-base levels (Station 11 along the Bafing, corresponding to the upper Senegal River; Figures 1a and 5a). (a) Google Earth view (left) with its geomorphic interpretation (right). (b) Cross-section drawn on Figure 3a showing the distribution of lateritic paleolandsurface relicts and the method by which they are projected or extrapolated above today's river courses.

Figure 4. Distribution of the optimum inverse concavity σ_{op} in the exponential fits of pediment surfaces 3 and 4.

Figure 5. Reconstructed paleo- and modern river long profiles and corresponding incision rates. For each river group, the case of the most representative river is shown. (a) Northwestern rivers (group A). (b) Short southern rivers (group B). (c) Long southern rivers (group C). (d) Low Niger River (group D). (e) High Niger River (group D). Paleoprofiles 2 are overestimated in elevation. Rivers and river groups are located on Figure 1a. The complete set of river long profiles may be found in the data repository.

Figure 6. Synthetic representation of the successive West African paleo-long river profiles. (a) Northwestern rivers (group A). (b) Short southern rivers (group B). (c) Long southern rivers (group C). (d) Niger River (group D) (location of river groups on Figure 1a). Spiked segments of modern profiles correspond to > 300 km long upward-convex segments (mapped in Figure 9). Elevation ranges of the lower and upper regional knickzones are shown in grey and numbered 1 and 2, respectively.

Figure 7. Statistical summary (box and whiskers plots) of incision rates over West Africa during periods III, IV and V (24-11, 11-6 and 6-0 Ma, respectively) for each river group. Incision rates III are maximum values (see text for explanation). Incision rates IV and V are calculated using the mean elevation of base levels 3, 4 and 5 where available. Note that incision rates for period V may be slightly underestimated, particularly on the lower course of rivers C and D, where a small number of stations are available on profile 4 but where locally large incision V occurs around modern knickzones.

Figure 8. Type evolutions of long river profile segments comprised between two stationary knickzones (grey vertical stripes) and corresponding finite incision patterns (vertical arrows). 1 – early river profile (green); 2 – late river profile (orange). (a) Parallel evolution by uniform incision. (b) Knickpoint creation by downstream rejuvenation. (c) Knickpoint creation by differential incision. (d) Slope decrease from incision gradient.

Figure 9. Distribution of the main anomalies in the modern river long profiles of West Africa and its interpretation in terms of long-wavelength lithospheric deformation of mantle origin. Red arrows represent directions of horizontal propagation of the uplift wave. Northeastward extensions of the Romanche (R) and St-Paul (SP) fracture zones constitute the two main transform segments of the continental margin.

*Highlights (for review)

Highlights:

- Reconstructed long profiles calibrate very slow incision (5 m/my) since Oligocene
- Profiles pinned-down at divide, outlet and stationary lithogenic knickzones
- Flexural uplift / dynamic topography mapped from profiles convexities & anomalies

Keywords:

River long profiles; incision dynamics; knickzones; non-orogenic; Cenozoic; Africa

Graphical Abstract (for review)

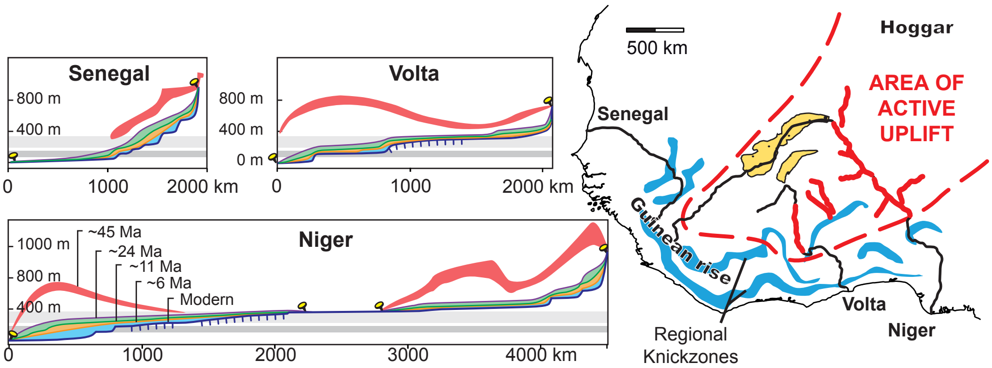

Figure 1
Click here to download Figure: Fig1.pdf

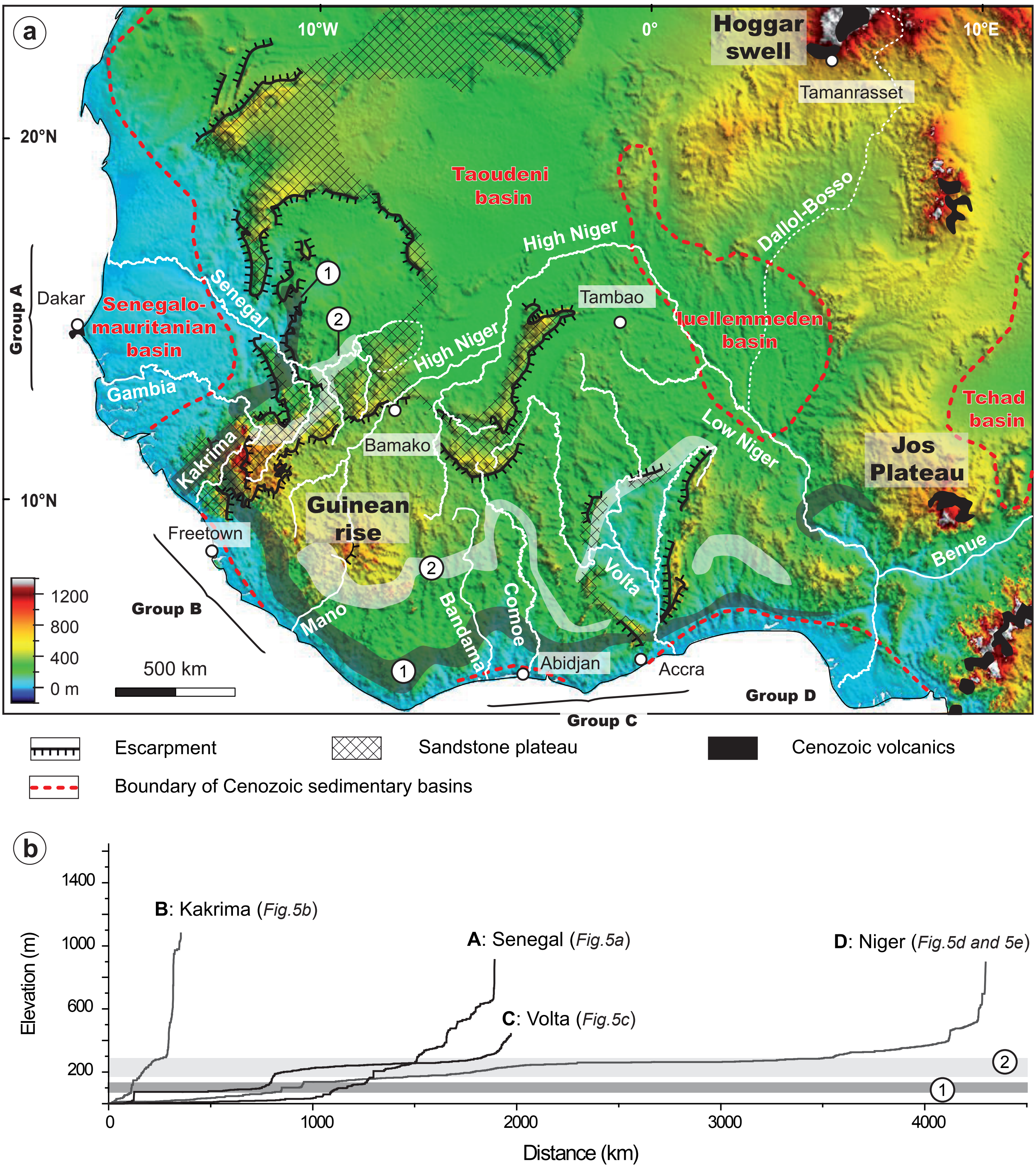

Grimaud et al., Figure 1

Figure 2
Click here to download Figure: Fig2.pdf

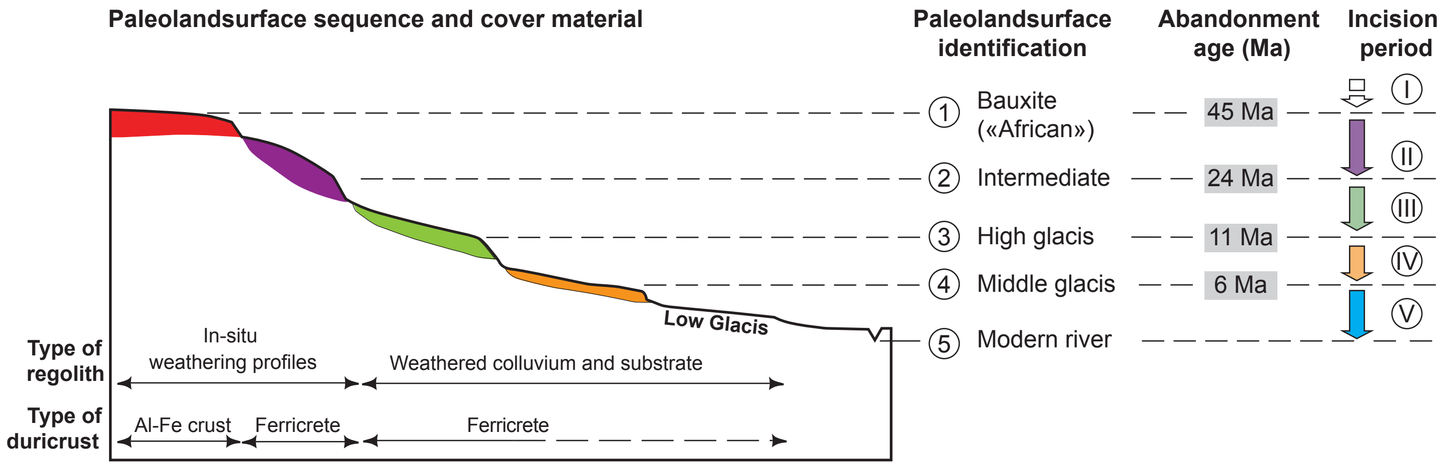

Grimaud et al., Figure 2

Figure 3

Click here to download Figure: Fig3.pdf

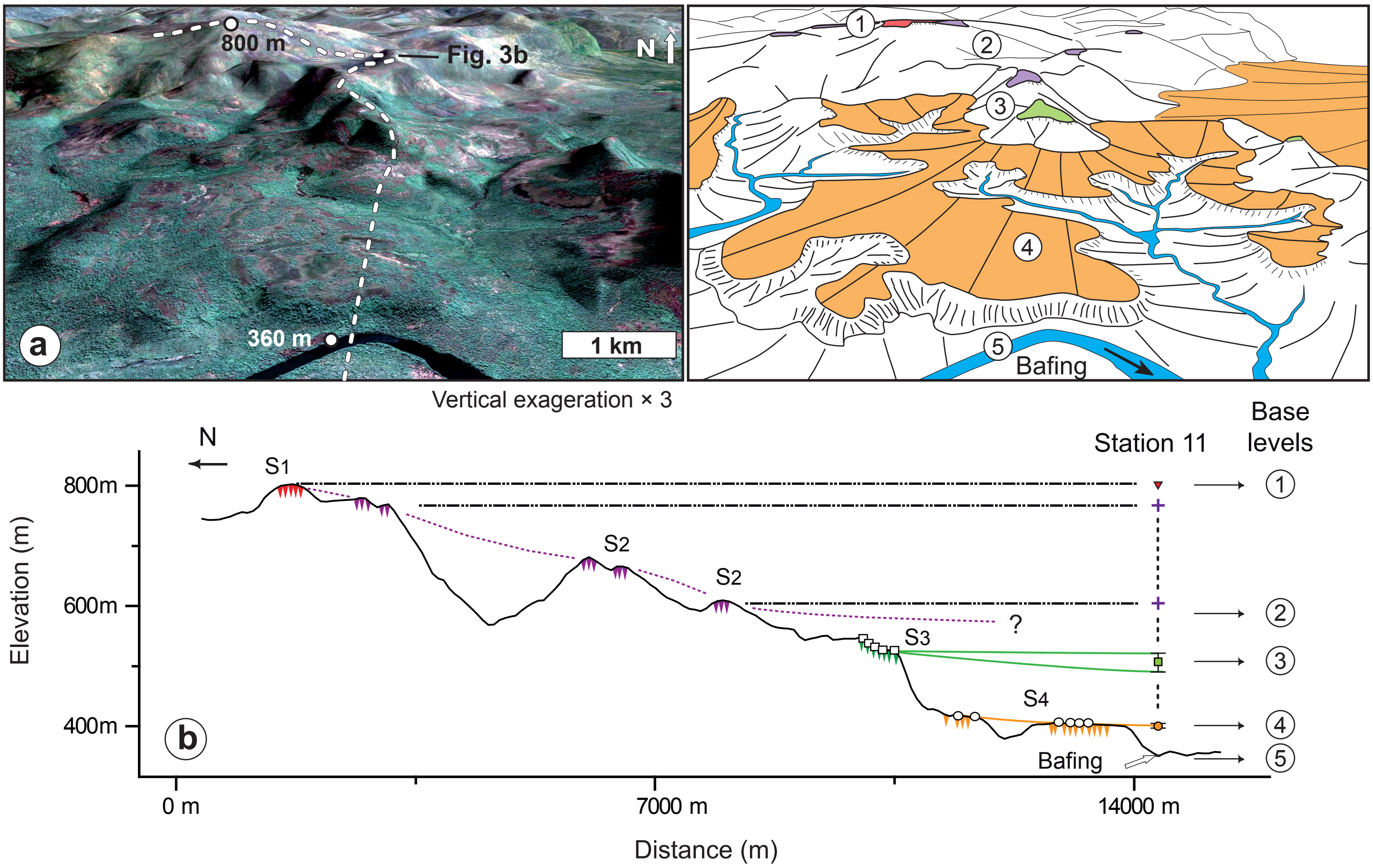

Grimaud et al., Figure 3

Figure 4
Click here to download Figure: Fig4.pdf

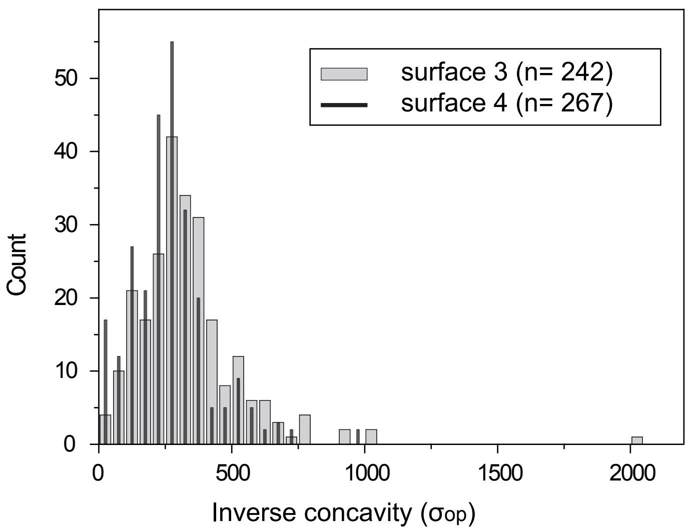

Grimaud et al., Figure 4

Figure 5
Click here to download Figure: Fig5.pdf

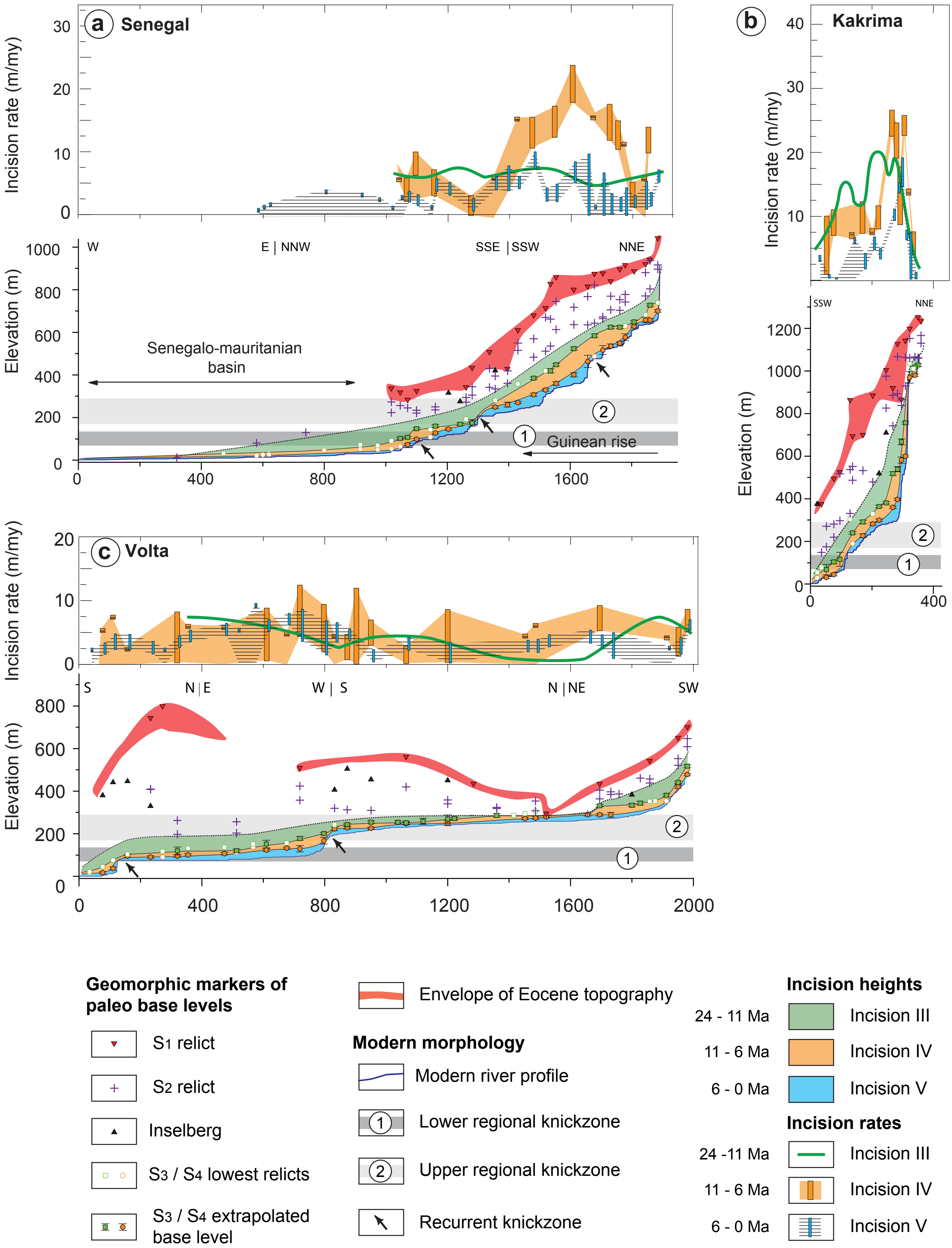

Grimaud et al., Figure 5

Figure 5, continued

Click here to download Figure: Fig5bis.pdf

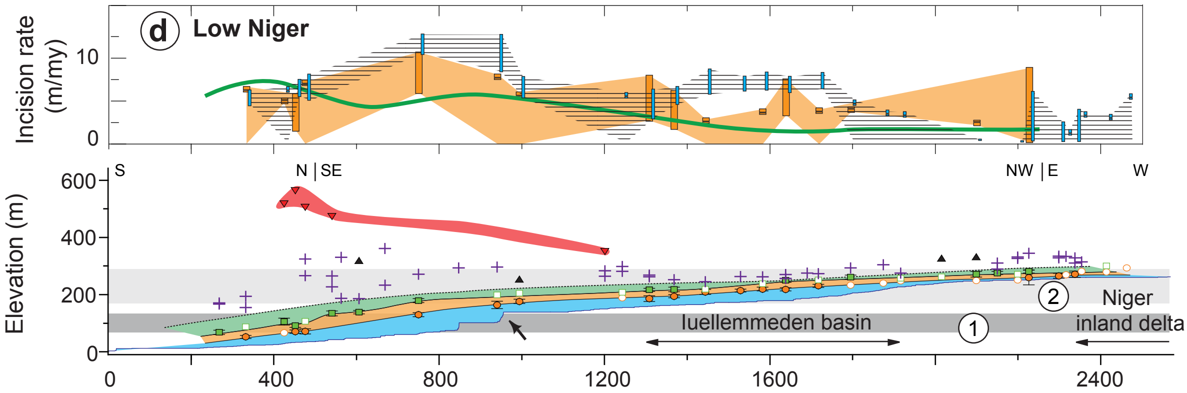

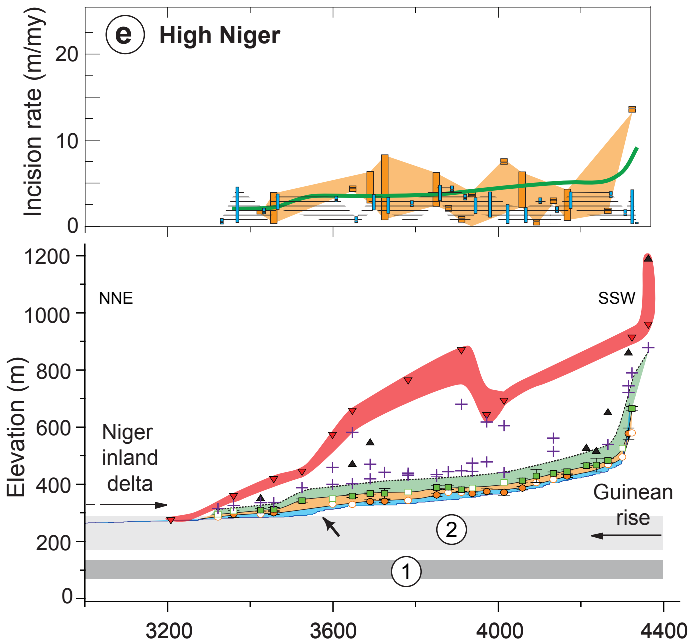

Grimaud et al., Figure 5 continued

Figure 6

Click here to download Figure: Fig6.pdf

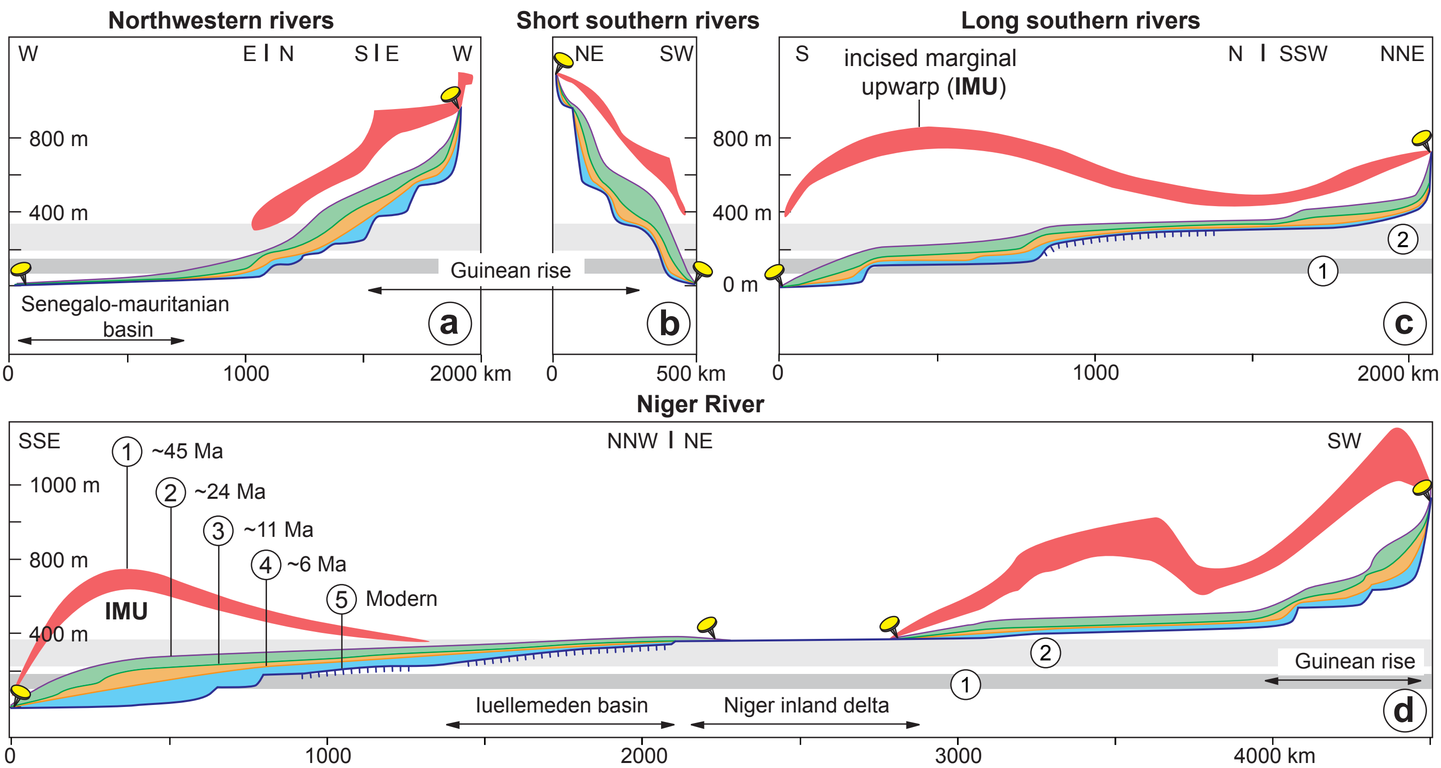

Grimaud et al., Figure 6

Figure 7
Click here to download Figure: Fig7.pdf

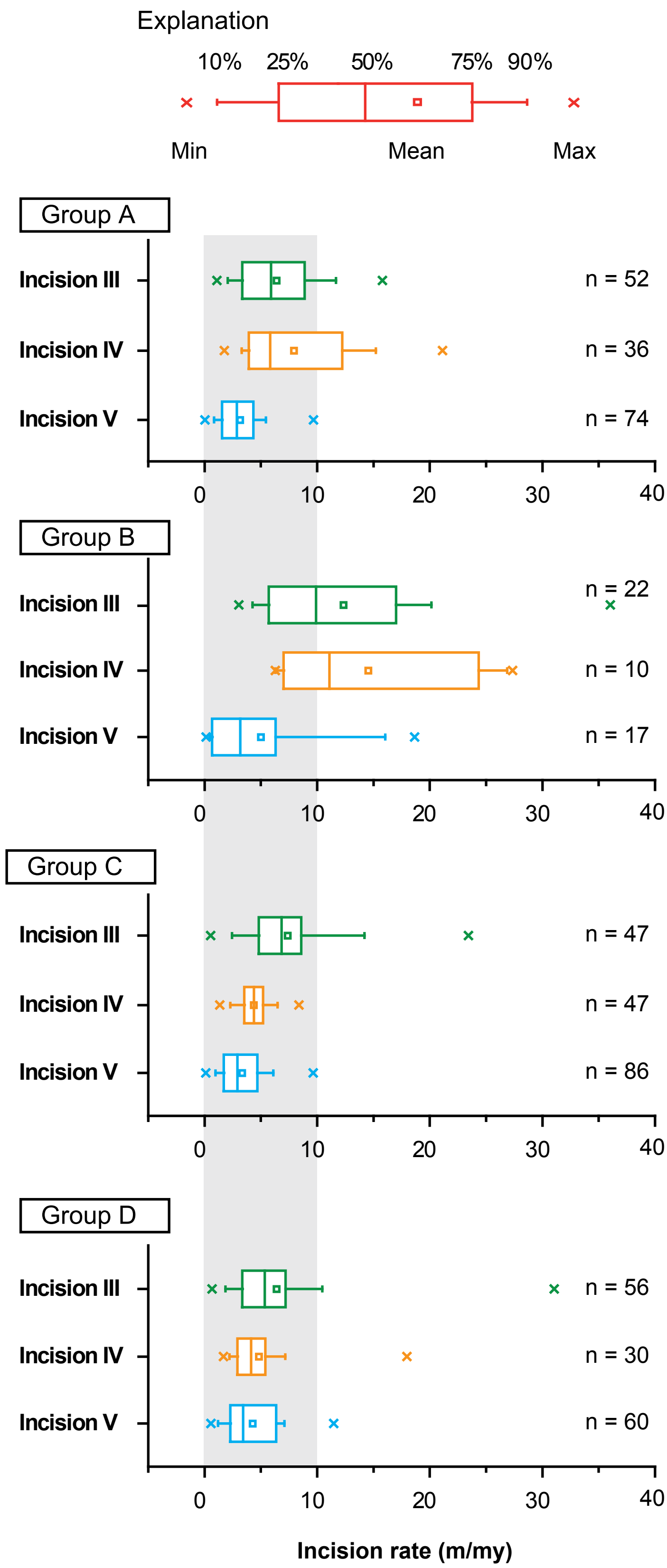

Grimaud et al., Figure 7

Figure 8
Click here to download Figure: Fig8.pdf

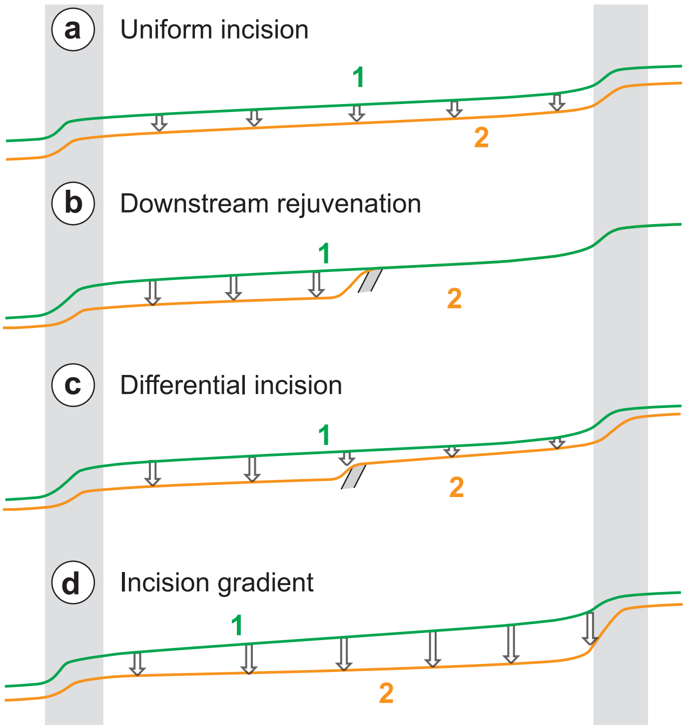

Grimaud et al., Figure 8

Figure 9
Click here to download Figure: Fig9.pdf

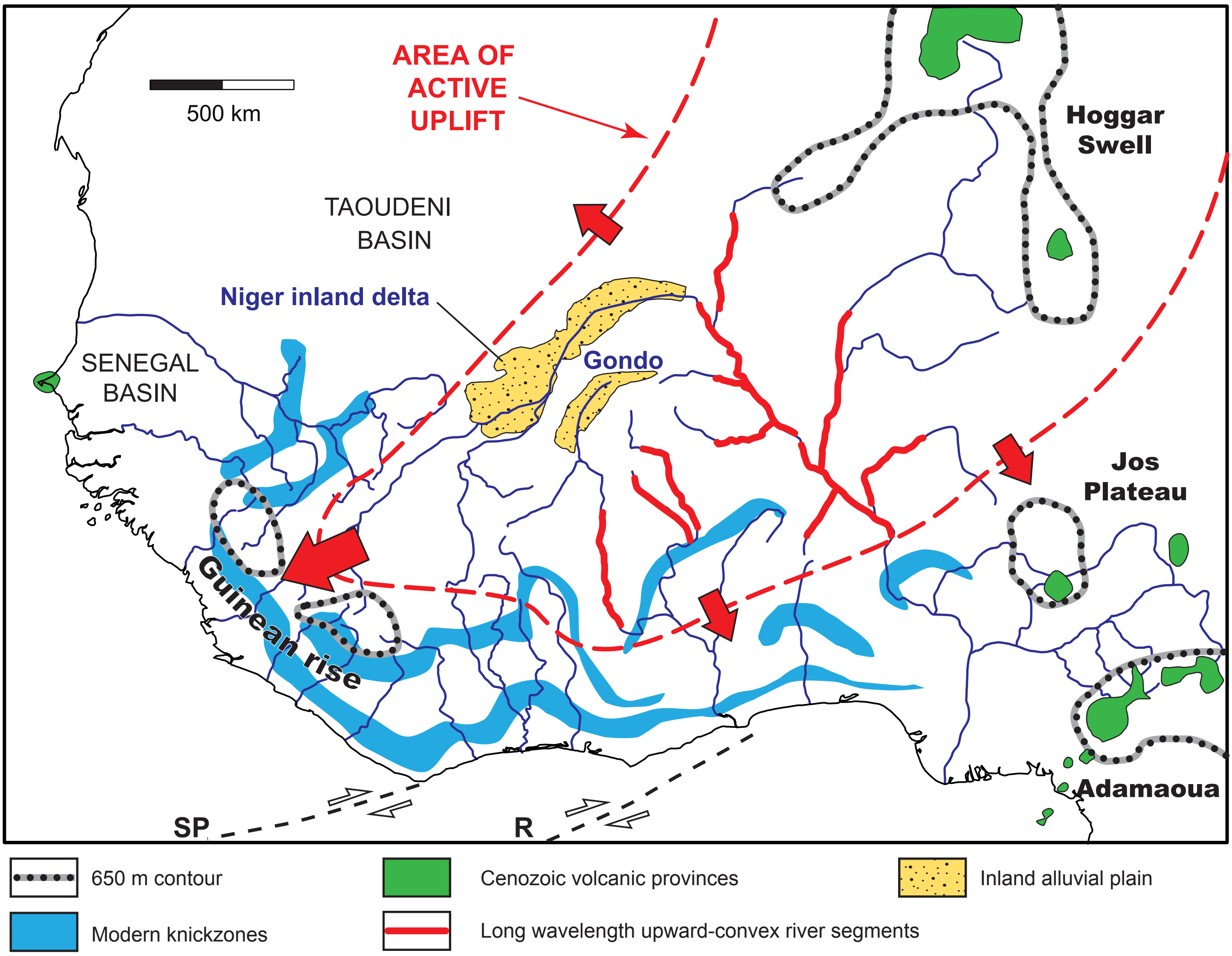

Grimaud et al., Figure 9